A Comparative Study and Performance Assessment of H °° Control Design

O'Young, Siu D.; Hope, J.; Åström, Karl Johan; Postlethwaite, Ian

1988

Document Version:
Publisher's PDF, also known as Version of record

CODEN: LUTFD2 / (TFRT-7403) / 1–32 / (1988)

A Comparative Study and Performance Assessment of H^∞ Control Design

S. D. O'Young
J. Hope
K. J. Åström
I. Postlethwaite

Department of Automatic Control
Lund Institute of Technology
October 1988

Department of Automatic Control
Lund Institute of Technology
P.O. Box 118
S-221 00 Lund Sweden

Document name
Report

Date of issue
October 1988

Document Number
CODEN: LUTFD2/(TFRT-7403)/1-32/(1988)

Author(s)
S.D. O'Young, J. Hope, K.J. Åström, I. Postlethwaite

Supervisor

Sponsoring organisation

Title and subtitle
A Comparative Study and Performance Assessment of H^∞ Control Design.

Abstract

This paper assesses the robust stability and robust performance properties of different H^∞ methods, and reports the use of a generalized two-input (vector) and two-output (vector) plant configuration in multivariable H^∞ design. Two industrial design examples are used: a scalar robot arm and a multivariable generation station and grid model. The H^∞ designs attempted tend to be conservative due to the representation of plant uncertainty as (H^∞) norm bounded perturbations neglecting the phase information, and the merging of multiple design objectives into one H^∞ norm. Despite the conservatism, the H^∞ approach is still systematic and useful for multivariable designs.

Key words

Classification system and/or index terms (if any)

Supplementary bibliographical information

ISSN and key title

ISBN

Language
English

Number of pages
32

Recipient's notes

Security classification

A Comparative Study and Performance Assessment of H^∞ Control Designs[$]

by

S.D. O'Young,[*] J. Hope,[§] K.J. Åström[†] and I. Postlethwaite[‡]

Abstract

This paper assesses the robust stability and robust performance properties of different H^∞ methods, and reports the use of a generalized two-input (vector) and two-output (vector) plant configuration in multivariable H^∞ design. Two industrial design examples are used: a scalar robot arm and a multivariable generation station and grid model. The H^∞ designs attempted tend to be conservative due to the representation of plant uncertainty as (H^∞) norm bounded perturbations neglecting the phase information, and the merging of multiple design objectives into one H^∞ norm. Despite the conservatism, the H^∞ approach is still systematic and useful for multivariable designs.

Keywords:

H^∞ Design, Robustness, Multivariable, Computer-Aided-Design, Industrial Applications

---

[$] The research is supported by the Science and Engineering Research Council, U.K.

[*] Dept. of Electrical Engineering, the Univ. of Toronto, Toronto, Ontario, M5S 1A4 Canada

[§] Central Electricity Generating Board, Barnwood, GL4 7RS, England, U.K.

[†] Dept. of Automatic Control, Lund Institute of Technology, Box 118, S-221 00 Lund 42, Sweden

[‡] Dept. of Engineering, Univ. of Leicester, Leicester, LE1 7RH, England, U.K.

1. INTRODUCTION

The objective of this paper is to report and assess the application of H^∞ optimization in control system design, with two industrial examples: a robot arm and an electrical power generation station. The robot arm is a scalar system with large variations in plant dynamics over its operating range. It is chosen to assess the robust stability and robust performance properties of the H^∞ method. The classical Horowitz and Sidi (1972) method is then compared against H^∞. The power station has 2 actuator inputs, 2 sensor signals, and 2 disturbance sources (one of which enters the plant neither via the actuator nor the sensor). It is chosen to demonstrate the use of a generalized two-input (vector) and two-output (vector) plant configuration in multivariable H^∞ optimization-based design. For implementation, the dominant dynamics of the multivariable H^∞ controller are identified, and the state-space H^∞ controller is subsequently reduced to classical PI controllers with constant cross-coupling terms.

In H^∞ designs, robust performance and robust stability requirements are specified as bounds on the weighted H^∞ norms of individual closed-loop transfer function matrices. These matrices are augmented (e.g. by stacking) into one single transfer function matrix, and a stabilizing contoller is found to minimize the H^∞ norm of this augmented matrix. The combination of multiple design objectives into one often gives conservative results because the H^∞ norm on the augmented matrix only imposes an upper bound on its elements. A sample of designs using this approach can be found in Postlethwaite (1986, 1987a) and Safonov (1986). Doyle (1983) proposes the use of μ analysis and synthesis methods to alleviate this conservatism essentially by solving a multiobjective optimization problem. Designs using the μ approach have been reported by Doyle (1986, 1987) and Fan (1987).

This paper deals only with H^∞ designs but not μ designs because the H^∞ optimization techniques are now well understood (Francis, 1987). All the H^∞ computations can be carried out in state-space (Doyle, 1988 and Chu 1986) and they have been implemented in H^∞ Computer-Aided Design (CAD) packages such as **Stable-H**[1] (Postlethwaite, 1987b) and LINF (Chiang, 1987). For μ, there

[1] All the design examples in this paper have been carried out using this CAD package, at Oxford University, England, U.K.

does not appear to be an efficient algorithmic implementation of the synthesis procedure and there are no CAD packages available.

This paper differs from other application papers on H^∞ design in that it offers a tutorial introduction as well as an assesment of the methodology. The tutorial introduction is made possible by abstracting the algorithmic implementation of H^∞ optimization as a 'black box' OPT procedure [2]. Design rules for weights selection are introduced, and the H^∞ design results are then assessed by comparison with the classical Horowitz method (Horowitz and Sidi, 1972). A complete multivariable design cycle from engineering specifications to implementation considerations is also reported. We begin by introducing the use of H^∞ optimization in controller design in the next section.

2. H^∞ DESIGN PROCEDURE

The plants used in this assessment have all been modelled as linear time invariant, continuous time and lumped parameter systems which have both state-space realizations and transfer function matrix representations in the Laplacian variable s: $G = \begin{bmatrix} A & B \\ C & D \end{bmatrix}$ and $G(s) = C(sI - A)^{-1}B + D$. The system G is said to be *stable* if the state matrix A has no eigenvalues in the closed right-half-plane. Suppose G is stable; then the H^∞ norm of G can be defined via its transfer function matrix representation as $\|G\|_\infty = \sup_\omega \overline{\sigma}[G(j\omega)]$, where $\overline{\sigma}[G(j\omega)]$ denotes the largest singular value of G at frequency ω. When G is scalar, its H^∞ norm is simply the highest gain on its Bode plot. We also use the symbol RH^∞ to denote matrices with stable real-rational entries in s, that is, the real-rational subspace of H^∞.

2.1 Formulation of Control System Designs as H^∞ Optimizations

The general compensation configuration used in this assessment is shown in Fig. 1. It will, in the sequel, be referred to as the Standard Compensation Configuration (SCC). The objective is

[2] The interested reader is referred to Chu (1986), Francis (1987) and Doyle (1988) for its implementation details. An understanding of the OPT procedure is not assumed nor needed to read this paper.

to design a compensator K (in state-space form), usually known as the controller, for the plant P (represented also in state-space form) such that the input/output transfer characteristics from the external input vector d to the external output vector e is desirable, according to some engineering specifications. The internal compensation signal flow paths are represented by vectors y and u, and correspond to the sensor signals and actuator demands, respectively.

The compensated system (that is, with the controller K in the internal signal path) shown in Fig. 1 is said to be *internally stable* if the augmented A matrix of the compensated system is stable. In other words, when the external signal $v = 0$, the states of both P and K will go to zero asymptotically for any initial conditions. Such a controller is said to be *stabilizing.*

Let M denote the closed-loop transfer function matrix mapping external input v to external output e, and let W_i and W_o be weights in RH^∞, chosen to emphasize (or de-emphasize) the relative importance of the external input and output signal. The H^∞ approach is to design a controller K such that the H^∞ norm of M is minimized. In other words, the objective is to solve the following optimization problem

$$\min_{K \text{ stabilizing}} \|W_o M W_i\|_\infty \ , \qquad OPT$$

where the minimization is over *the whole set* of stabilizing controllers.

3. AN INDUSTRIAL ROBOT ARM

A simple model (Åström *et al.*, 1987) of a robot arm is used in the assessment of the robustness properties of the H^∞ method. The transfer function from the control input (motor current) to measurement output (motor angular velocity) is

$$P_{Ja}(s) = \frac{km\,[Ja\,s^2 + d\,s + k]}{(s + p_1)\,[Ja\,Jms^2 + d\,(Ja + Jm)s + k\,(Ja + Jm)]} \qquad (1)$$

where $Ja \in [.0002,\ 0.002]$, $Jm = 0.002$, $d = 0.0001$, $k = 100$, $km = 0.5$ and $p_1 = 0.01$ [3]. The moment of inertia Ja of the robot arm varies with the arm angle. Bode plots of the plant gain for the extreme values of the arm inertia Ja in (1), where $P_o := P_{Ja=0.002}$ and $P_e := P_{Ja=0.0002}$, are given in Fig. 2.

Since this robot arm plant has large variations in dynamics over its required operating range of angular positions, the objective is to design a robust controller which is insensitive to these variations and exhibits good tracking and disturbance rejection properties at all angular positions. The ability to maintain stability over the entire range of plant dynamic variations is referred to as *robust stability* (RS) and the ability to stay, at the same time, within certain performance requirements is referred to as *robust performance* (RP). We also use the term *nominal performance* (NP) to refer to the performance of the closed-loop system pertaining to a nominal plant.

The most general fixed gain compensation configuration for satisfying both tracking and disturbance rejection requirements is a two-degree-of-freedom controller, consisting of an inner loop for robust stability and disturbance rejection, and an outer loop for tracking. We will concentrate mainly on the inner loop design. A pre-compensator consists of a simple first-order lag, acting as a set-point scheduler, is adequate.

Three approaches are undertaken in this comparative study: two H^∞ designs, one aiming at achieving robust performance and robust stability simultaneously, the second at only simultaneous nominal performance and robust stability, and the third a classical design via the Horowitz method. The plant uncertainty for the H^∞ designs is modelled as (H^∞) norm-bounded additive perturbations on a nominal plant, and for the Horowitz method as real parameter (Ja) perturbations.

[3] The small constant p_1 is added to avoid the Model Matching Transformation zero (O'Young, 1989) caused by a pole at the origin. This small perturbation is not needed if we are prepared to solve a fully specified but more complex H^∞ design problem.

3.1 Robust Performance and Robust Stabilization via H^∞ Optimization

Our treatment of the robust performance and robust stability requirements follows Doyle's (1984) method of representing these design requirements as an unstructured additive perturbation to the nominal plant. Consider the inner-loop compensation configuration in Fig. 3 where P_o is the nominal plant and K is the inner-loop feedback compensator, Δ_1 and Δ_2 are additive perturbations, representing plant uncertainty and performance requirements respectively, and W_1 and W_2 are weights. We assume that Δ_1 and Δ_2 are scaled via W_1 and W_2 such that they are closed unit-balls ($:= \{\delta \in RH^\infty : \|\delta\|_\infty < 1\}$) in RH^∞.

For robust performance, suppose that the variations in dynamics from the nominal plant are contained within a filtered unit-ball in RH^∞:

$$\{W_2\,\delta : \delta \in \Delta\} \supset \{P - P_o : P \in \mathcal{P}\}, \tag{2}$$

where $\mathcal{P} := \{P_{Ja} : Ja \in [0.0002,\ 0.002]\}$, and P_o is the nominal plant. Then a sufficient condition for robust stability is that K stabilizes the set of plants $\{P_o + W_2\,\delta : \delta \in \Delta_2\}$ which, by (2), contains $\mathcal{P}$.

Define the sensitivity function S_p as $S_p := (1 + PK)^{-1}$ and a robust performance requirement can be defined as $\forall P \in \mathcal{P}$ and $\forall \omega \in \Re$, $|S_P(j\omega)|\ |W_1(j\omega)| < 1$. In other words, the disturbance rejection ratio ($:= d/e$, Fig. 3) is guaranteed, over all possible $P \in \mathcal{P}$, to be bigger than $|W_1|$ at all frequencies.

To represent the requirments for robust performance and robust stability simultaneously in the OPT setting, the closed-loop transfer function matrix is defined as

$$M := \begin{bmatrix} W_1\,S_{P_o} \\ W_2\,K\,S_{P_o} \end{bmatrix}. \tag{3}$$

The following robust performance and robust stability sufficiency result is then obtained.

RPRS *Controller K satisfies the robust performance and robust stability requirements if (i) K stabilizes P_o and (ii) $\|M\|_\infty < 1/\sqrt{2}$.*

Proof: For robust stability, we have $\forall\ \delta_1 \in \Delta_1$ and $\forall\ \delta_2 \in \Delta_2$, since Δ_1 and Δ_2 are unit-balls in RH^∞, $\|[\delta_1,\ \delta_2]\|_\infty \leq \sqrt{2}$. By (i), M is stable, and $\forall \delta_1 \in \Delta_1$ and $\forall \delta_2 \in \Delta_2$, we have $\|[\delta_1,\ \delta_2]M\|_\infty \leq \|[\delta_1,\ \delta_2]\|_\infty \|M\|_\infty < 1$. The small gain theroem then implies that the interconnected system in Fig. 3 is stable. For robust performance, suppose $\exists\, \delta_2 \in \Delta_2$ and $\exists\, \omega \in \Re$ such that $|(S_{P_o+\delta_2} W_1)(j\omega)| \geq 1$. Then, there exists a real-rational function $\delta_1 \in \Delta_1$ with the appropriate gain and phase shift such that $(S_{P_o+\delta_2} W_1 \delta_1)(j\omega) = 1$. The unity-gain positive feedback would destabilize the interconnected system, and hence contradicts the robust stability condition. **Q.E.D.**

To achieve RPRS for the robot arm example, the SCC plant corresponding to the closed-loop transfer function matrix M in the OPT problem is constructed by interconnecting the state-space realizations of P_o, W_1 and W_2 according to Fig. 3. Weight W_2 is chosen to satisfy Inequality 2; in particular, it is constructed as a stable real-rational function such that $\forall P \in \mathcal{P}$ and $\forall \omega \in \Re$,

$$|W_2(j\omega)| > |(P - P_o)(j\omega)|\,. \tag{4}$$

Weight W_1 is a high-gain low-pass filter with the highest possible cross-over frequency ω_c ($:= \omega : |W_1(j\omega)| = 1$) chosen iteratively such that the solution to the OPT problem is achievable at a cost less than $1/\sqrt{2}$.

The sensitivity functions corresponding to the nominal plants P_o and P_e are shown in Fig. 4. Note that the cross-over frequency ω_c for the final design is at 6 rad/sec, and that both $|S_{P_o}|$ and $|S_{P_e}|$ are both below 0 dB at 6 rad/sec. The robust performance requirement is thus achieved.

3.2 Nominal Performance and Robust Stabilization via H^∞ Optimization

The NPRS design requirements vary slightly from those of RPSP in the sense that robust stability is retained as an obvious hard design constraint, but optimal nominal performance is only required for the nominal plant. The rationale behind such a strategy is that if $|S_{P_o}|$ is made small enough over the operating band, the closed-loop dynamics within the inner loop should also be relatively

insensitive to plant perturbation, hence achieving robust performance indirectly (O'Young and Francis, 1986).

Consider again the compensated system in Fig. 3 with Δ_1 removed from the block diagram and let M in the OPT problem be defined as before in the RPRS case.

NPRS *Controller K satisfies the nominal performance and robust stability requirements if (i) K stabilizes P_o and (ii) $\|M\|_\infty < 1$.*

Proof: It follows, by (ii), $\|M\|_\infty < 1$ which implies that $\|W_2 K S_{P_o}\|_\infty < 1$. Since $\forall\, \delta_2 \in \Delta_2$, δ_2 is stable and $\|\delta_2\| \leq 1$, it follows by (i) and the small gain thereom that the interconnected system in Fig. 3 is stable. Nominal Performance follows immediately from (ii) since $\|W_1 S_{P_o}\|_\infty < 1$. **Q.E.D.**

The NPRS condition differs from the RPRS case only by raising the cost of the OPT problem by a factor of $\sqrt{2}$. In general, this number increases at the rate of $\sqrt{n}$ where n is the number of blocks of additive unstructured perturbations, representing both robust performance and robust stability requirements.

The design procedure follows exactly as in the RPRS case where W_2 is the same as before, and the highest achievable cross-over frequency ω_c for W_1 satisfying Inequality (ii) in the NPRS design is 15 rad/sec; hence 2.5 times higher than the achievable cross-over frequency of the RPRS design, although the actual bandwidths of S_{P_o} are similar in both case. This shows that a NPRS design can sometimes satisfy RPRS requirements because robust performance depends on nominal performance in most feedback designs. The sensitivity functions corresponding to P_o and P_e are shown in Fig. 4.

3.3 Robust Performance and Robust Stability via the Horowitz method

The H^∞ approach is often criticized for being conservative, and to demonstrate this fact, we present the result of Åström *et al.* (1987), on the same design via the Horowitz method. Horowitz deals with the RPRS requirements by characterizing the so-called Horowitz bounds on a set of discrete

frequency points $\{\omega\}$ over a frequency band, delimiting the feasible compensator complex gain regions B_ω, where

$$B_\omega := \{\alpha(\omega) : \left|\frac{1}{1+\alpha(\omega)P(j\omega)}\right| \leq x(\omega),\ \forall P \in \mathcal{P} \tag{5.1}$$

and

$$\left|\frac{\alpha(\omega)P(j\omega)}{1+\alpha(\omega)P(j\omega)}\right| \leq b(\omega) - a(\omega),\ \forall P \in \mathcal{P}\} \tag{5.2}$$

on a Nichols' chart. Condition 5.1 is a direct characterization of the complex inner-loop compensator gain needed to guarantee a disturbance rejection ratio $\geq 1/x$ over all possible plant dynamics $P \in \mathcal{P}$. Condition 5.2 is needed to guarantee the existence of an outer-loop controller such that the compensated frequency response for command signal tracking stays at the same time within the tolerance limits $b(\omega) - a(\omega)$. These tolerance limits are sometimes derived from time (step) response requirements for designs involving minimum phase plants. Note that the actual perturbed set of plants $\mathcal{P}$ is used in the characterization of B_ω, instead of a norm-bounded set (2) as in H^∞ design.

The inner-loop compensator K is synthesized by 'pasting' together, for example, by real-rational function approximations, so that its frequency response lies within the Horowitz bounds and satisfies the usual Nyquist stability condition. The sensitivity functions corresponding to P_o and P_e are shown in Fig. 4. Note that the disturbance rejection bandwidths are in the region of $50-100$ rad/sec, much higher than those achieved via the H^∞ methods.

3.4 Conservatism in the H^∞ Designs

The conservatism in the H^∞ designs stem mainly from the representation of plant uncertainty (2) and the formulation of a multi-objective optimization problem (3) as a single-objective OPT problem.

In the Horowitz method, both the gain and phase information on the plant dynamics variations are used in the characterization of feasible regions for the compensator frequency response. In the H^∞

design, we only use the gain information via Inquality 2 but ignore the phase information. Phase information can only be ignored at high frequencies where the sensor signal is often dominated and corrupted by noise which contains no deterministic phase information. Phase information is however important at low frequencies or in the cross-over (cut-off) frequency range, where perturbations are typically structured.

Because of the low-damping resonant peaks and troughs occurring at frequencies around 250-300 rad/sec and higher (Fig. 2), a sufficient condition for robust stability is to limit the inner-loop disturbance rejection bandwidth to be less than 250 rad/sec as demonstrated by the frequency responses of the H^∞ controllers as shown in Fig. 5. In fact, the optimal H^∞ controllers can be replaced by 4th-order low-pass filters with the respective cut-off frequencies with no appreciable change in closed-loop time responses. In the case of the Horowitz design, the controller gain can be kept high at frequencies beyond 250 rad/sec because phase information is used in the characterization of plant uncertainty.

Although the low-frequency gain of the Horowitz controller is also significantly higher than the H^∞ controllers, the high gain is not needed to reject output disturbance. The low-frequency gains of the H^∞ controllers can be increased, if necessary, by choosing higher low-frequency gain for W_1 without affecting the performance of the resultant design.

Since W_2 has to be synthesized by a real-rational function approximation to satisfy the Inequality 3, allowance must be made for approximation error. Fig. 6 shows the error margin of an eighth-order real-rational function approximation $|P_e - P_o|$, with the most pronounced error occurring at frequencies just below the resonant frequency of P_o at around 100-300 rad/sec. This error forces the H^∞ controllers to have lower gain bandwith than is actually constrained by Inequality 2.

In the RPRS design, the obvious conservatism comes from the requirement that $\|M\|_\infty$ be $< 1/\sqrt{2}$ which implies that $\|W_2\, K\, S_{P_o}\|_\infty$ must also be $< 1/\sqrt{2}$. It has however been shown in the NPRS case that $\|W_2\, K\, S_{P_o}\|_\infty < 1$ is already sufficient to guarantee robust stability.

In the NPRS design, the objectives $\|W_1 S_{P_o}\|_\infty < 1$ and $\|W_2 K S_{P_o}\|_\infty < 1$ must be satisfied simultaneously. These two objectives are imbedded into the single-objective OPT problem by stacking them as M (3). The two objectives are satisfied independently only if they are prescribed over disjoint frequency bands. This seldom happens for practical problems since they usually have nearly equal gain around the cross-over frequency band. The design requirement for the optimal NPRS design is that $|S_{P_o}| < 1$ at the cross-over frequency, but the actual gain is -3 dB because the robust stability condition constraint contributes also to the gain of M. In fact, the conservatism of the stacking and the error margin in the synthesis of W_2 is taken into account, the actual cost of the NPRS design can be pushed up to about 1.8 without violating either the nominal performance or the robust stability constraints.

3.5 The Outer-Loop Design

The design of the pre-compensator will be discussed briefly to complete the robot arm design. Tracking is an open-loop property when there is no plant uncertainty, and this is especially true if the inner loop has high enough gain such that the closed loop dynamics are sufficiently insensitive to variations in plant dynamics. This applies to our robot arm example, and the required outer-loop compensator is simply a first-order lag: $\frac{1}{1+\tau s}$. With τ chosen to be ≥ 0.03 second, the rate of change of the command signal fed to the inner loop is slow enough not to excite the lowest resonant frequency (around 300 rad/sec) of the robot arm at all angular positions. Fig. 7 shows the step responses of the various inner-loop designs for the extreme values of Ja. Note that the tracking response for the NPRS design with cost =1.8 acheives nearly the same speed as the Horowitz design for the nominal design, but the performance degrades significantly for the perturbed plant P_e.

4. A POWER GENERATION EXAMPLE

The power station shown in Fig. 8 is usually operated at full load and is tied to the load grid. The load frequency N (in % pu) is affected by the electrical power input from this station and by the external perturbation E_d (in % pu) on the load demand. The thermal power input to the boiler is

controlled by the flow rate of hot carbon dioxide gas circulated through the reactor. It is assumed that the hot gas temperature is kept constant by a relatively tight regulation of the reactivity via the reactor control rods. For this example, the hot gas feed rate is taken as the heat input Q (in % pu) to the boiler. The boiler steam pressure P_S (in bars) is influenced by Q and the throttle valve opening A_s (in % pu) which acts a speed governor for the turbine. The total perturbation to the boiler is modelled as additive steam perturbation P_d at the output. The measured outputs are N and P_S, and the actuator inputs are Q and A_s. The disturbance inputs are E_d and P_d. The design objective for the station control system is to suppress the disturbance of N from E_d and P_d, and to keep the variations of P_S within limits.

This example is used to demonstrate the use of H^∞ optimization for designing a controller in a generalized two-input (vector) and two-output (vector) SCC plant and the resulting H^∞ controller will then be simplified. Here, neither robust performance nor robust stability is a design concern, since we will consider operation at full power only with little variations in plant dynamics. Coordinated control of actuators Q and A_s for the best possible regulation of N is of primary interest. In other words, we are dealing with a nominal performance optimization problem.

4.1 A Multivariable H^∞ Design

The internal configuration of the SCC plant (see the Appendix for its state-space realization) is shown in Fig. 9. The external input vector $d := [E_d \; P_d]^T$ represents the disturbances to the power station and the external output vector $e := [N \; P_S \; Q \; A_s]^T$ represents the responses to be minimized. The actuator demands Q and A_s are included as constraints to prevent saturations in the case of large and abrupt disturbances. The internal feedback signal vector $y := [N \; P_S]^T$ and $u := [Q \; A_s]^T$ are signals provided for the control system from plant instrumentation. Let M be the transfer function matrix mapping the closed-loop external signals from d to e. The H^∞ design problem is formulated as an OPT problem to minimize the weighted H^∞ norm of M.

4.2 Weights Selection and Controller Design

Input weight W_i in OPT is used to scale the magnitudes of the worst-case E_d and P_d disturbances, and has been chosen to be a constant diagonal matrix of the form $W_i = \begin{bmatrix} 2 & 0 \\ 0 & 1 \end{bmatrix}$. Output weight W_o is chosen to be diagonal with entries w_1, w_2, w_3 and w_4 in RH^∞. Weights w_1 and w_2 are chosen to be low-pass filters with appropriate cut-off frequencies to represent the required disturbance rejection bandwidths from d to e. Weights w_3 and w_4 are high-pass filters representing the actual useful bandwidths of the actuators. The frequency responses of the weights for the final design are shown in Fig. 10.

The H^∞-optimal controller is obtained by solving the OPT problem iteratively, and trading off the relative bandwidths of w_1 and w_2 to achieve a satisfactory compromise between the regulation of N and P_S. The closed-loop response of e as the result of 2 % pu drop in power demand (E_d) is shown in Fig. 11. These results compare favourably with the existing station control system which consists of scalar proportional plus integral (PI) loops and constant feedforward terms.

4.3 Controller Simplication

The 'full order' controller from **Stable-H** has 15 states. It can be reduced to 6 states (see the Appendix) by the minimal realization procedure proposed by Tombs (1985) without appreciable changes in closed-loop responses. The resultant 2×2 6-state controller still has 64 parameters and is still considered to be too complex for implementation. It is desirable to simplify this controller by identifying its dominant modes and algebraic couplings so that it can be implemented using conventional PI control loops.

By using elementary row and column operations on the B, C and D matrix of a state-space realization of the 6-state controller K and observing the Nyquist plots and step responses of its scalar elements, the controller is diagonalized at low frequencies. The dominant dynamics of the low-frequency model of the controller consists, in fact, of two PI terms as shown in Fig. 12. By adding a further second-order term whose resonant frequency and damping ratio correspond to the

complex conjugate pair of eigenvalues (at $s = -.49 \pm j0.83$) of the A matrix of the original state-space controller K, the frequency and steps responses of the simplified controller match closely with those of the state-space model except for the very fast transient modes. It is felt that the high-frequency dynamics of the H^∞ controller should be dropped because it is neither desirable nor useful to excite the power station with fast control actions.

The closed-loop responses to the same 2 % pu drop in E_d corresponding to the simplified controller are almost identical to the 6th-order state-space model. The second order term can also be replaced by a constant gain 1, resulting in slightly faster transient responses, at the risk of reaching actuator rate limits for large (and abrupt) disturbances in E_d.

5. CONCLUSIONS

The optimization of robust performance and robust stability can be formulated as an H^∞ design problem but with a conservative result. Alternatively, one can optimize nominal performance and can check *posteriori* whether or not the nominal design meets the robust performance as well.

With the robot arm example, we have identified and demonstrated two major sources of conservatism in H^∞ design: the representation of (real-parameter) plant perturbations by norm-bounded uncertainty and the inadequacy of a single-objective H^∞ OPT problem to represent multiple design objectives. Doyle's μ approach addresses these problems, and should become a powerful CAD tool when a numerically reliable and efficient μ synthesis procedure is available. At present, numerical optimization based CAD packages such as Boyd's (1988) qdes and Polak's (1982) DELIGHT can also handle multiple design objectives, specified both in time and frequency domains.

For scalar and minimum phase systems, an experienced designer can usually do better with classical techniques than resorting to the arsenal of a norm-based optimization method like H^∞. For multivariable systems, despite its conservatism, the systematic H^∞ optimization is however a viable and attractive design tool, as demonstrated by the power-station example. An optimization based

technique can give a reasonable preliminary design on which refinements can be added to satisfy additional design objectives such as time domain performance which cannot be included directly in H^∞.

It should be emphasized that we have only used an additive perturbation for modelling plant uncertainty in the robot arm example. Other representations such as stable factor perturbations (Vidyasagar, 1985) might model the actual plant uncertainty more accurately and make the resulting H^∞ design less conservative. Futhermore, H^∞ designs are highly sensitive to the choice of weights. It is not claimed that the H^∞ design is the best achievable. A challenging exercise could be to find other weights and models of plant uncertainty for improving the H^∞ designs for the robot arm.

The two-input two-output SCC approach is a natural structure in multivariable designs where disturbances, control variables, actuator inputs and sensor outputs originate at different locations of the plant. The most general setting is to consider the controller to be also in the SCC form (Nett, 1986 and Desoer, 1987) thus allowing a disturbance signal to be added to the controller. A controller synthesis procedure in this setting needs to be considered.

The approximation of a state-space controller obtained from a norm-based optimization procedure such as H^∞ by a simple and structured one as in Section 4.3 is needed to economize on hardware and software implementation costs. Also and perhaps more importantly, gain scheduling (e.g. for start-up and shut-down) nonlinear characteristics (e.g. reset wind-up) and integrity behaviour (e.g. loss of sensor signals) may be more intuitive and hence more manageable. The simplification procedure is usually done on an ad-hoc trial-and-error basis, and this needs to be performed within a user-friendly CAD environment.

ACKNOWLEDGEMENT

The authors would like to thank the Central Electricity Generating Board in the United Kingdom for permission to publish this paper.

REFERENCES

Åström, K., L. Neumann and P. Gutman (1986). A comparison of robust and adaptive control. *Proc. 2nd IFAC Workshop on Adaptive Syst. Contr. and Signal Processing*, Lund, Sweden, 37.

Boyd, S.P., V. Balakrishnan, C.H. Barratt, N.M. Khraishi, X. Li, D.G. Meyer and S.A. Norman (1988). A new CAD method and associated architectures for linear controllers. *IEEE Trans. Auto. Cont.*, **AC-33(3)**, 268.

Chiang R.Y. and M.G. Safonov (1987). The LINF computer program for L^∞ controller design. *Univ. of Southern Calif. Report*, **EECG-0785-1**.

Chu, C.C., J.C. Doyle and E.B. Lee (1986). The general distance problem in H^∞ optimal control theory. *Int. J. Control*, **44**, 565.

Desoer C.A. and A.N. Gündes (1987). Algebraic theory of linear time-invariant feedback systems with two-input two-output plant and compensator. Electronic Research Laboratory, UC Berkeley, **UCB/ERL M87/1**.

Doyle J., K. Glover, P. Khargonekar and B. Francis (1988). State-space solution to standard H_2 and H_∞ control problems. *Proc. American Cont. Conf.*, Atlanta, GA.

Doyle, M. Morari, R.S. Smith, A. Skjellum, S. Skogested and G.J. Ballas (1987). Case study session: applications of multivariable robust control techniques. IFAC World Congress, Munich, FRG.

Doyle, J.C. (1984). Lecture notes in advances in multivariable control. *ONR/Honeywell Workshop*, Minneapolis, MN.

Doyle, J.C. (1983). Synthesis of robust controllers and filters with structured plant uncertainty. *Proc. IEEE Conf. Dec. Control*, 109.

Francis, B. (1987). A Course in H_∞ Control Theory. Springer.

Horowitz, I. and M. Sidi (1972). Synthesis of feedback systems with large plant ignorance for prescribed time-domain tolerances. *Int. J. Control*, **16(2)**, 287.

Nett, C.A. (1986). Algebraic aspects of linear control system stability. *IEEE Trans. Auto. Cont.*, **AC-31(10)**, 941.

O'Young, S.D., I. Postlethwaite and D.-W. Gu (1989). A treatment of model matching zero in the optimal H^2 and H^∞ control design. To appear in *IEEE Trans. Auto. Cont.*.

O'Young, S.D. and B.A. Francis (1986). Optimal performance and robust stabilization. *Automatica*, **22**, 171.

Polak E., P. Seigel, T. Wuu, W. Nye and D. Mayne (1982). DELIGHT.MIMO: an interactive, optimization-based multivariable control system design package. *IEEE Contr. Syst. Mag.*, 4.

Postlethwaite I., S. O'Young, D.-W. Gu and J. Hope (1987a). H^∞ control system design: a critical assessment based on industrial applications. *Proc. IFAC World Congress*, Munich, FRG.

Postlethwaite I., S. O'Young and D.-W. Gu (1987b). **Stable-H** User's Guide. *Univ. of Oxford*, **OUEL 1687/87.**

Postlethwaite I., D.-W. Gu, S. O'Young and M. Tombs (1986). Industrial control system design using H^∞ optimization. *Proc. IEEE Conf. Dec. Control*, 12.

Safonov, M.G. and R.Y. Chiang (1986). CACSD using the state-space L^∞ theory – a design example. *Proc. IEEE Conf. on CACSD.* Washington, DC.

Tombs, M.S. and I. Postlethwaite (1987). Truncated balanced realization of a stable non-minimal state-space system. *Int. J. Control.*

Vidyasagar, M. (1985). Control System Synthesis, a factorization approach. MIT Press, Cambridge, Ma.

CAPTIONS FOR FIGURES

Fig. 1: The Standard Compensation Configuration

Fig. 2: Bode Plots of P_o and P_e

Fig. 3: RPRS Design Configuration

Fig. 4: Bode Plots of S_{P_o} and S_{P_e} for Robot Arm Designs

Fig. 5: Bode Plots of the Controllers for Robot Arm Designs

Fig. 6: Approximation of Plant Uncertainty by W_2

Fig. 7: Step Responses for Robot Arm Designs

Fig. 8: Power Generation Station

Fig. 9: SCC Plant for the Power Generation Example

Fig. 10: Bode Plots of Weights for the Power Generation Station Example

Fig. 11: Step Response to 2 % pu Increase in E_d

Fig. 12: Simplified H^∞ Controller

$$PI1 = \frac{-(1.1+12s)}{s}, \quad PI2 = \frac{0.016}{s}$$

$$OR2 = \frac{1}{s^2/\omega_n^2 + 2\zeta s/\omega_n + 1} \text{ where } \omega_n = 0.96 \text{ and } \zeta = 0.5.$$

$K1 = -30$, $K2 = -0.5$, $K3 = 0.8$ and $\begin{bmatrix} Q \\ A \end{bmatrix} = \begin{bmatrix} 1 & -0.3 \\ 2.1 & 0.37 \end{bmatrix} \begin{bmatrix} Q' \\ A' \end{bmatrix}$.

The power station SCC plant:

A =

-0.1000d-03	0.3900d-01	0.5635d-04	0.0000d+00
0.0000d+00	-0.1425d+00	0.7318d-03	0.0000d+00
0.0000d+00	0.0000d+00	-0.2049d-01	0.4000d+01
0.0000d+00	0.0000d+00	0.0000d+00	-0.1000d+00

B =

0.5000d-03	0.0000d+00	0.0000d+00	0.7748d-04
0.0000d+00	0.0000d+00	0.0000d+00	0.1006d-02
0.0000d+00	0.0000d+00	0.0000d+00	-0.2817d-01
0.0000d+00	0.0000d+00	0.1000d-02	0.0000d+00

C =

0.1000d+03	0.0000d+00	0.0000d+00	0.0000d+00
0.0000d+00	0.0000d+00	0.8197d+00	0.0000d+00
0.0000d+00	0.0000d+00	0.0000d+00	0.0000d+00
0.0000d+00	0.0000d+00	0.0000d+00	0.0000d+00
0.1000d+03	0.0000d+00	0.0000d+00	0.0000d+00
0.0000d+00	0.0000d+00	0.8197d+00	0.0000d+00

D =

0.0000d+00	0.0000d+00	0.0000d+00	0.0000d+00
0.0000d+00	0.1000d+01	0.0000d+00	-0.4730d+00
0.0000d+00	0.0000d+00	0.1000d+01	0.0000d+00
0.0000d+00	0.0000d+00	0.0000d+00	0.1000d+01
0.1000d-02	0.0000d+00	0.0000d+00	0.0000d+00
0.0000d+00	0.1000d+01	0.0000d+00	-0.4730d+00

The reduced Controller:

A =

-0.2535d-02	0.2196d-03	-0.9558d-01	0.8878d-03	-0.1053d-02	-0.2007d-02
0.1235d-04	-0.1040d-03	0.3421d-01	-0.1367d-02	0.1294d-02	0.1284d-02
-0.1063d+00	-0.1887d-02	-0.5071d+02	-0.3560d+01	-0.8380d+00	-0.2120d+01
0.1997d-02	0.7848d-04	0.4653d+01	-0.2251d-01	0.6284d-01	0.4437d-01
0.1796d-02	-0.3645d-03	0.1911d+01	-0.6312d-01	-0.4877d-01	0.4043d-01
0.2031d-02	-0.1883d-03	0.2387d+01	-0.5835d-01	-0.1422d+00	-0.7481d-01

B =

0.1878d+01	-0.2924d-02
-0.1102d-01	-0.1052d+00
0.4019d+02	0.2415d-02
-0.7459d+00	-0.4287d-01
-0.6629d+00	-0.6089d-01
-0.7485d+00	0.2793d-01

C =

-0.7885d+00	0.9528d-01	0.4041d+00	0.7465d+00	-0.6543d+00	-0.4175d+00
-0.1705d+01	0.4592d-01	-0.4019d+02	0.3174d-01	-0.1226d+00	-0.6219d+00

D =

-0.1500d+01	-0.8739d-04
-0.8110d+01	-0.4723d-03

Open-Loop Poles:

No.	Real	Imag.
1	-50.25263	
2	-0.5100887	
3	-0.4935145e-01	0.8278035e-01
4	-0.4935145e-01	-0.8278035e-01
5	-0.2479007e-02	
6	-0.9987098e-04	

Finite Transmission Zeros:

No.	Real	Imag.
1	-186.2554	
2	-1.085320	
3	-0.1379847	0.6432413e-01
4	-0.1379847	-0.6432413e-01
5	-0.1665605e-01	

Appendix

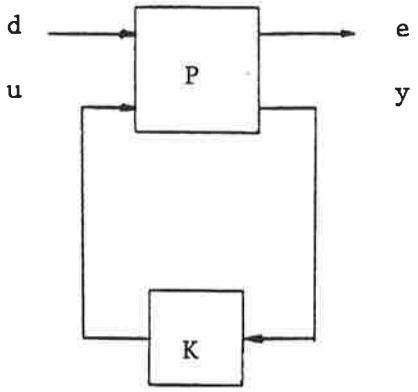

Fig.1

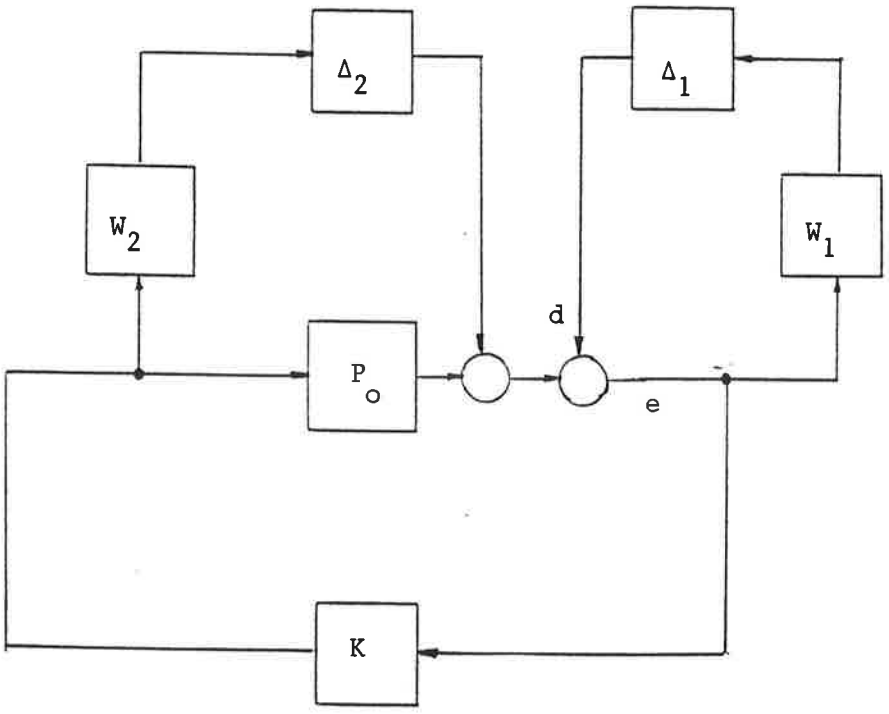

Fig. 3

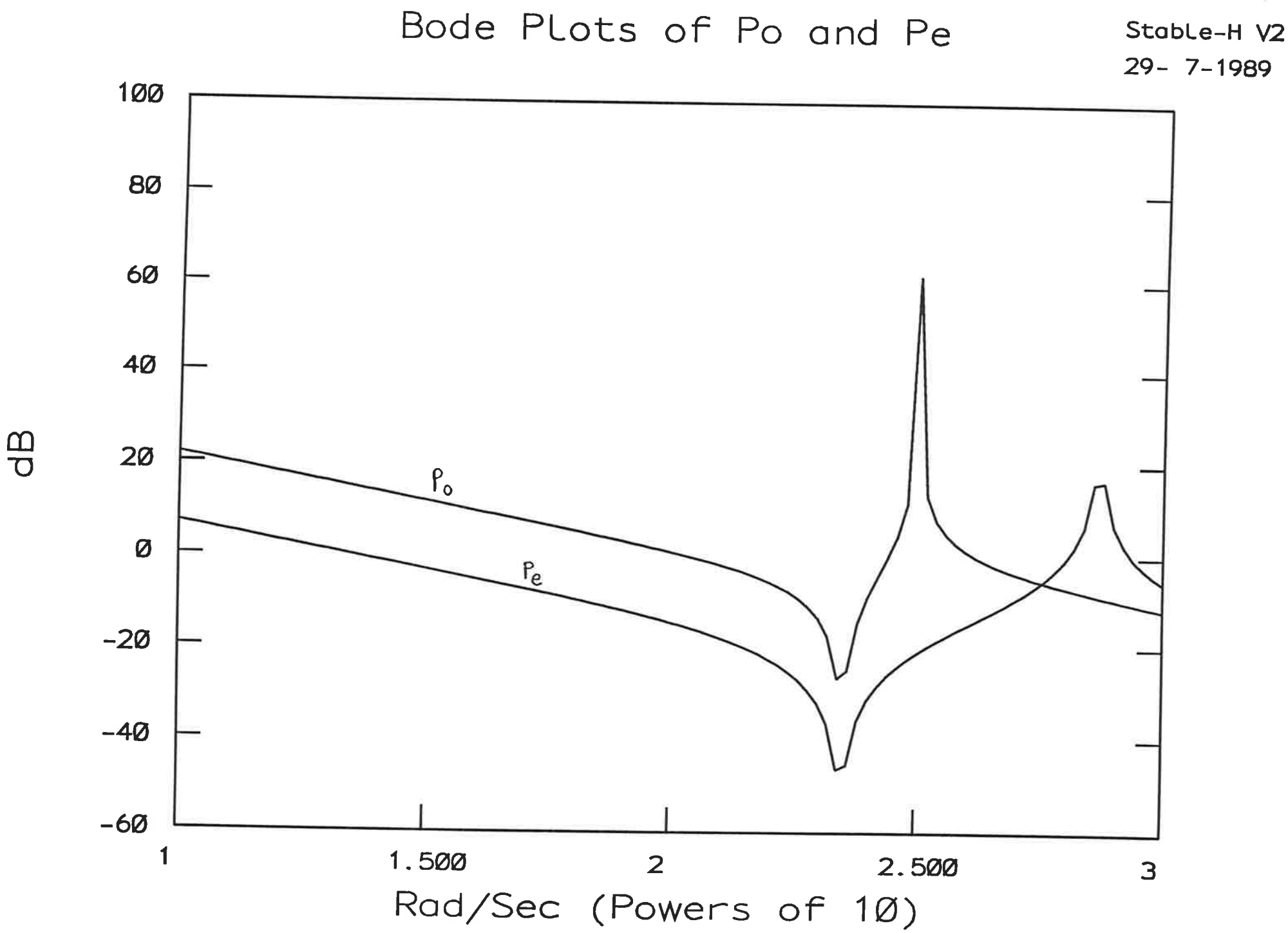
Bode Plots of Po and Pe
Stable-H V2
29- 7-1989
100
80
60
40
20
0
-20
-40
-60
dB
Po
Pe
1
1.500
2
2.500
3
Rad/Sec (Powers of 10)

Fig. 2.

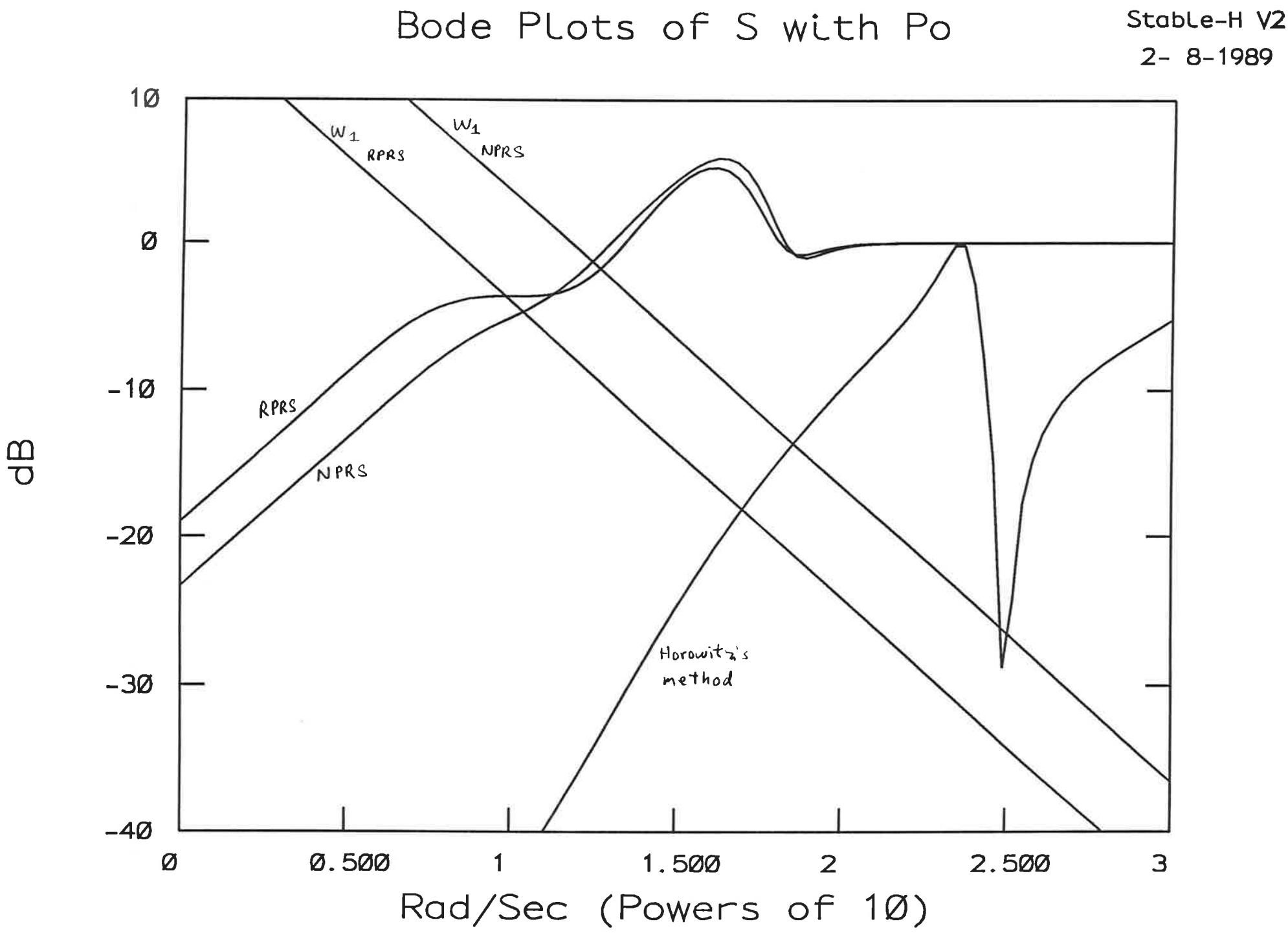
Bode Plots of S with Po
Stable-H V2
2- 8-1989
10
0
-10
-20
-30
-40
dB
W1
RPRS
W1
NPRS
RPRS
NPRS
Horowitz's
method
0
0.500
1
1.500
2
2.500
3
Rad/Sec (Powers of 10)

Fig 4 a

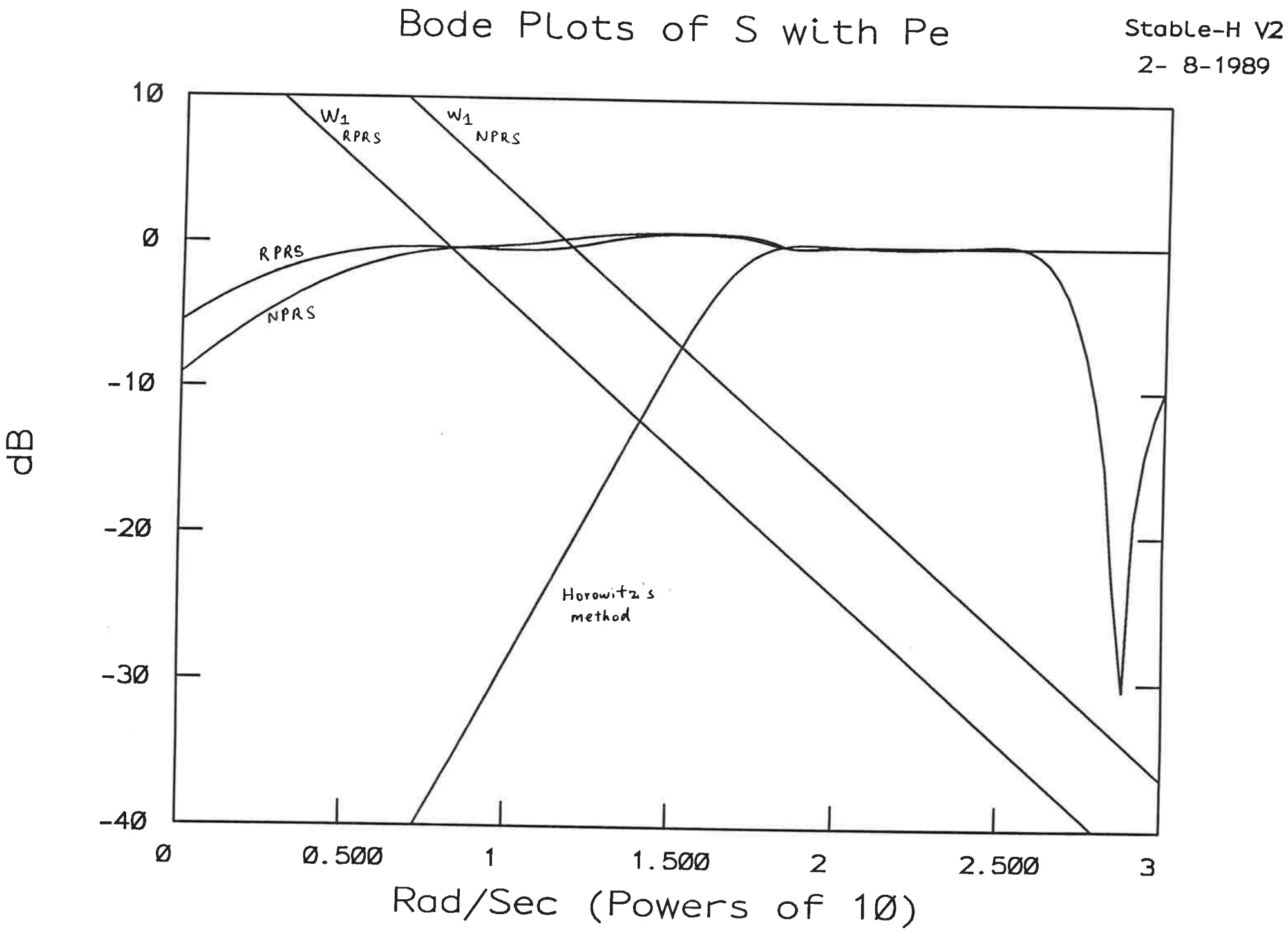
Bode Plots of S with Pe
Stable-H V2
2- 8-1989
10
0
-10
-20
-30
-40
dB
W1 RPRS
W1 NPRS
RPRS
NPRS
Horowitz's method
0
0.500
1
1.500
2
2.500
3
Rad/Sec (Powers of 10)

Fig. 4 b

Bode Plot of Inner Controllers

Stable-H V2
29- 7-1989

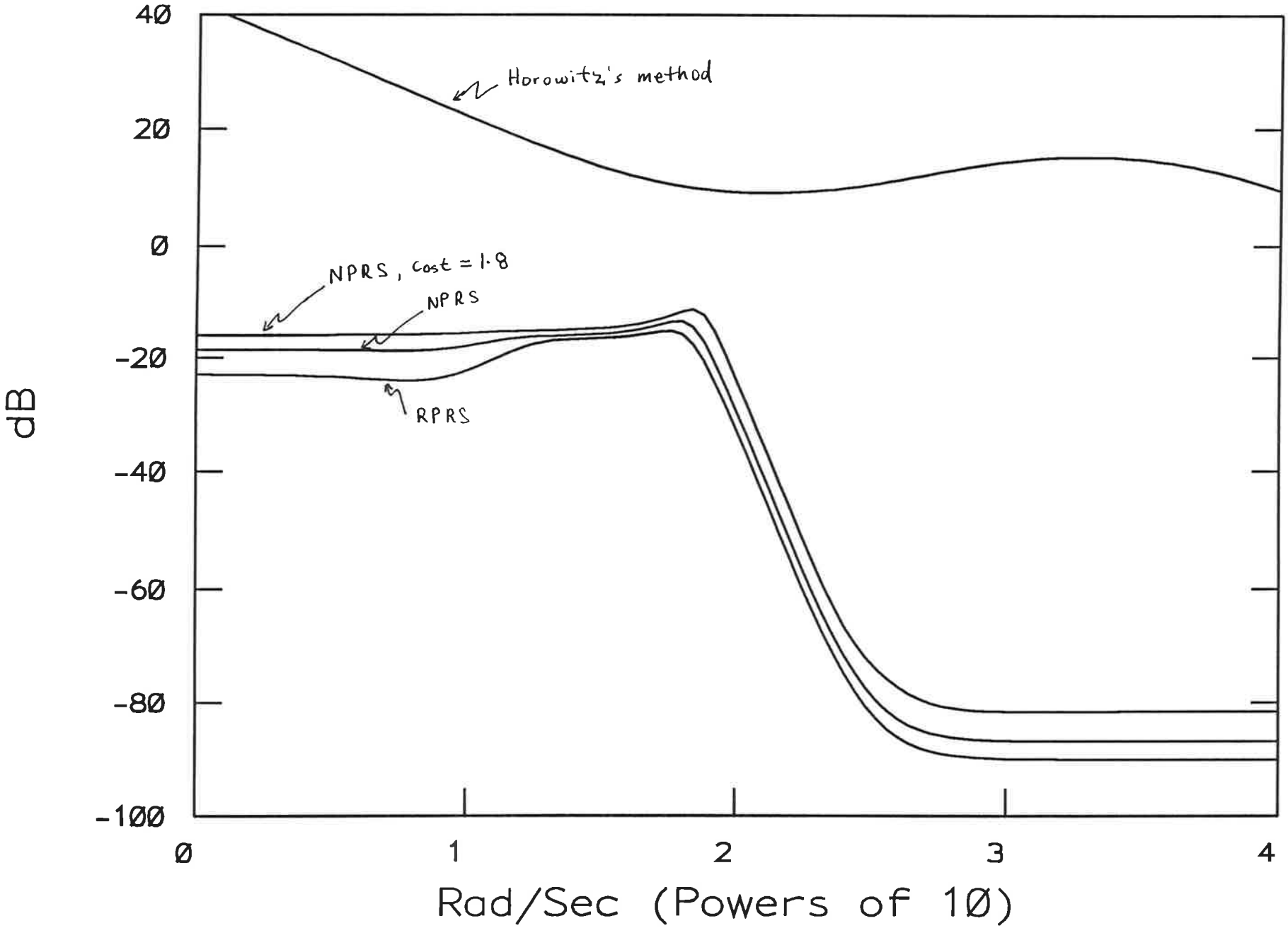

Fig. 5

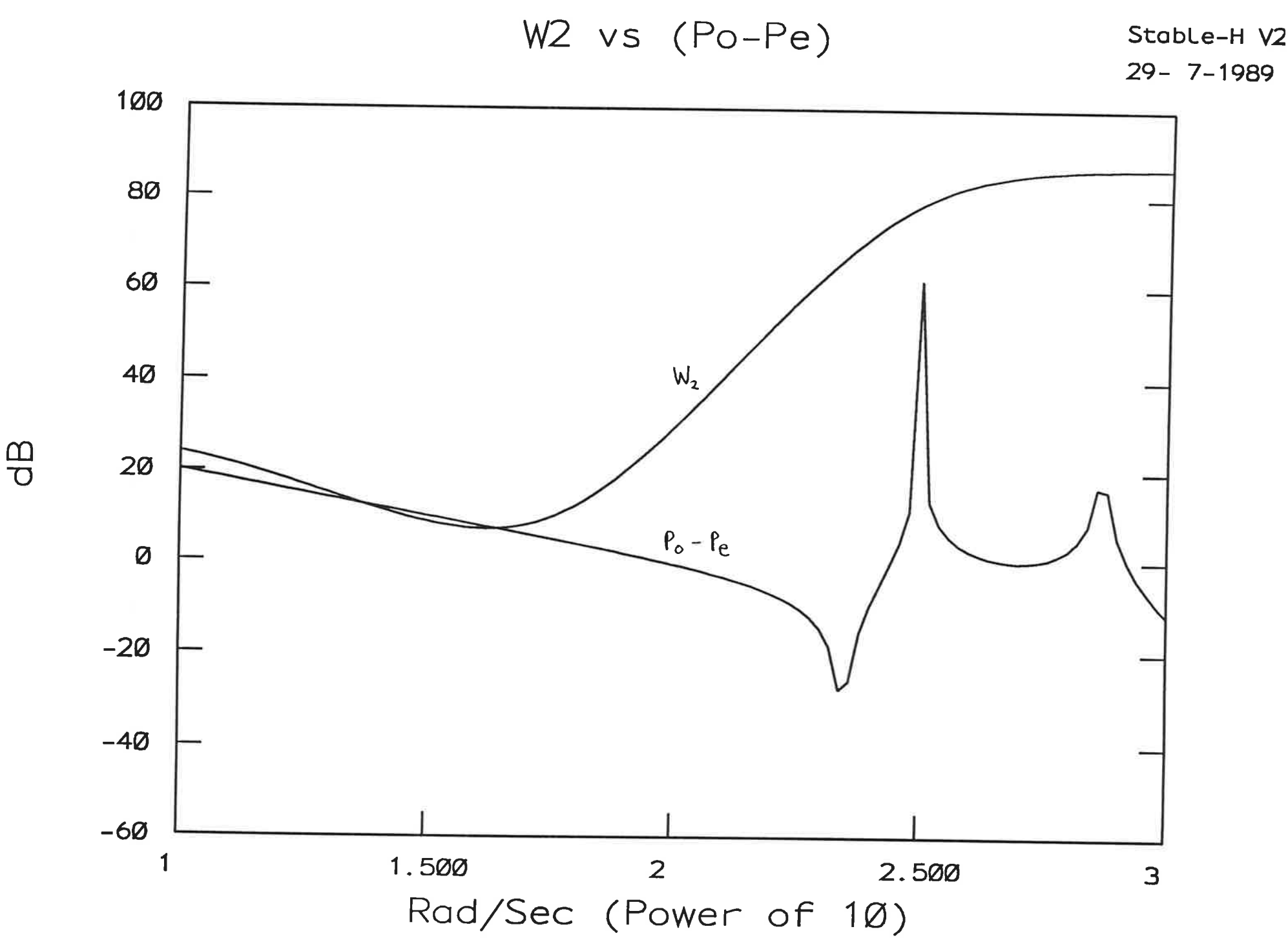
W2 vs (Po-Pe)
Stable-H V2
29- 7-1989
100
80
60
40
20
0
-20
-40
-60
dB
W_2
$P_o - P_e$
1
1.500
2
2.500
3
Rad/Sec (Power of 10)

Fig. 6

Step Responses for Robot Arm

Stable-H V2
29- 7-1989

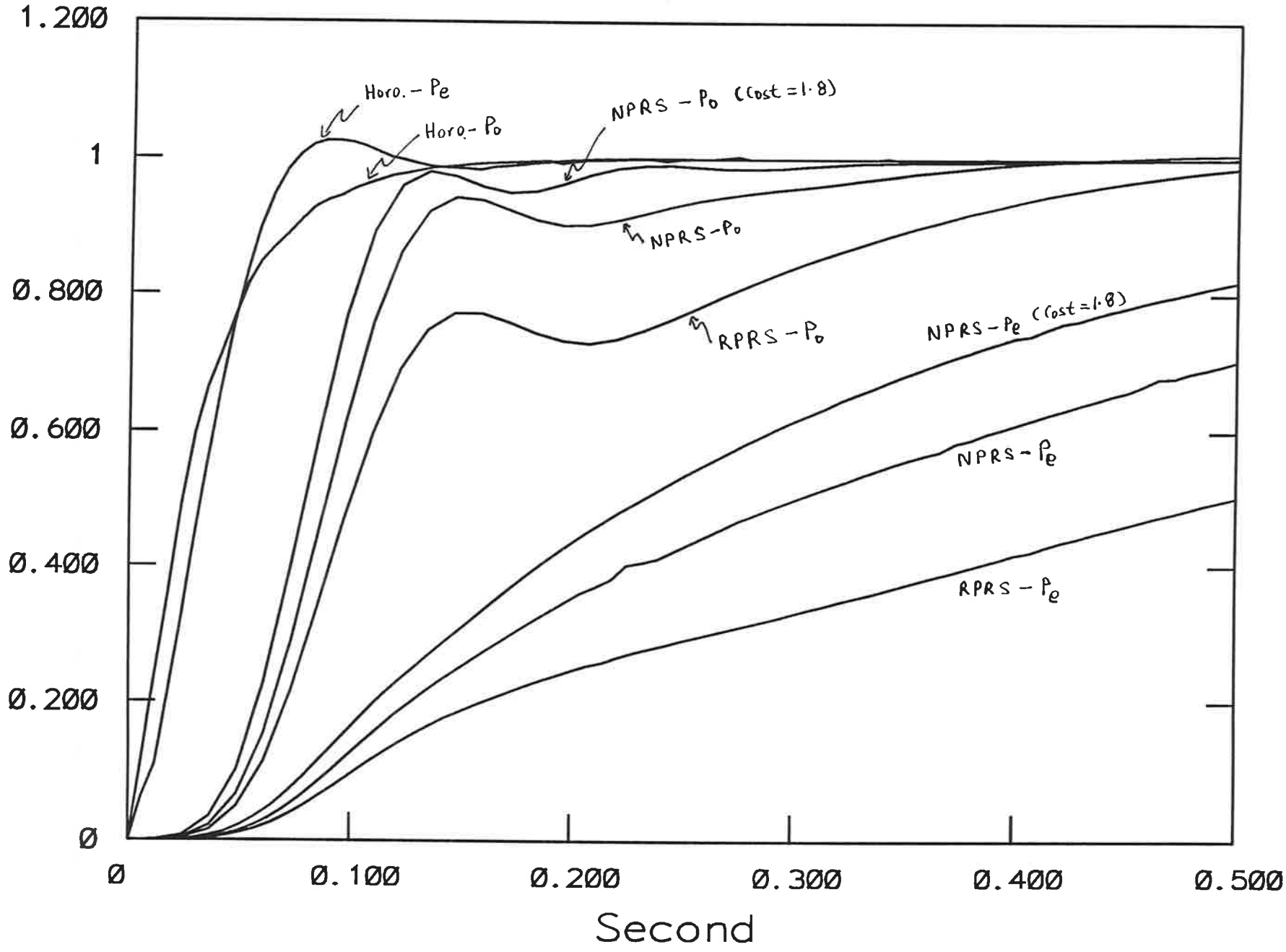

Fig. 7.

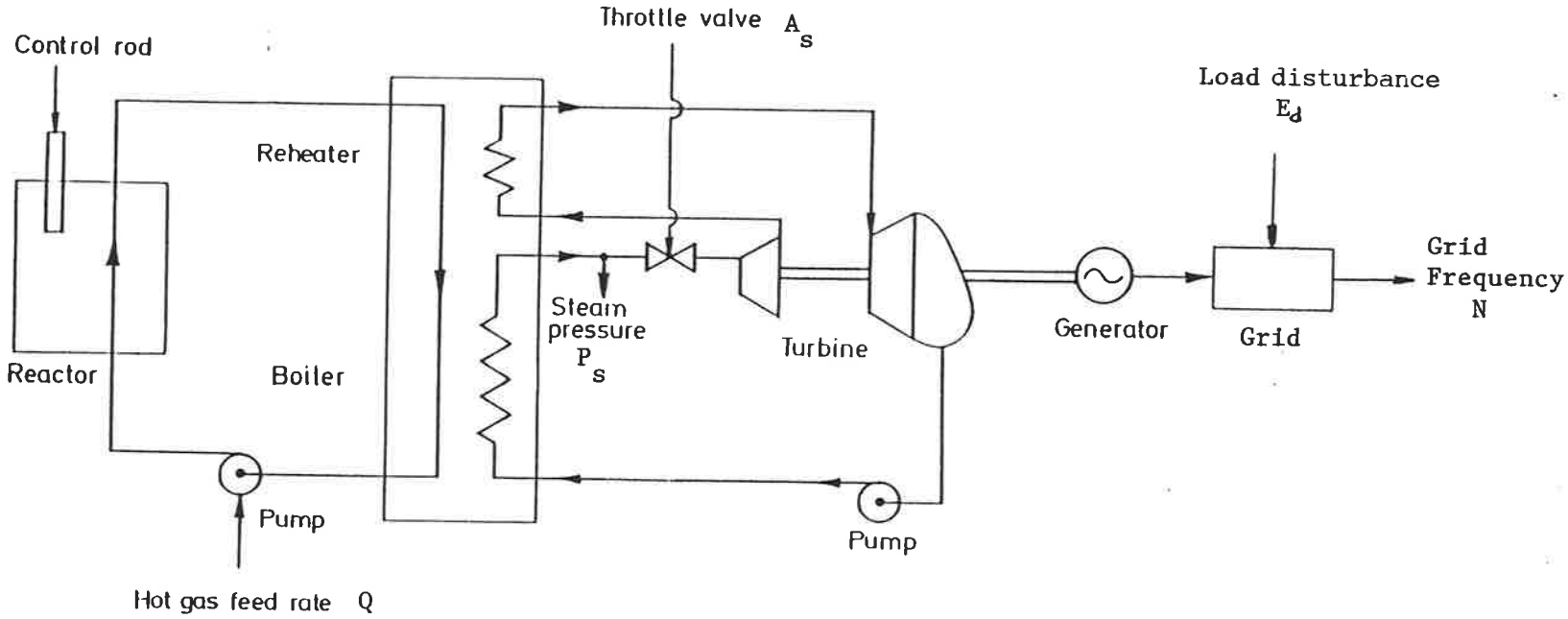
Control rod
Throttle valve A_s
Load disturbance
E_d
Reheater
Steam
pressure
P_s
Grid
Frequency
N
Reactor
Boiler
Turbine
Generator
Grid
Pump
Pump
Hot gas feed rate Q

Fig. 8.

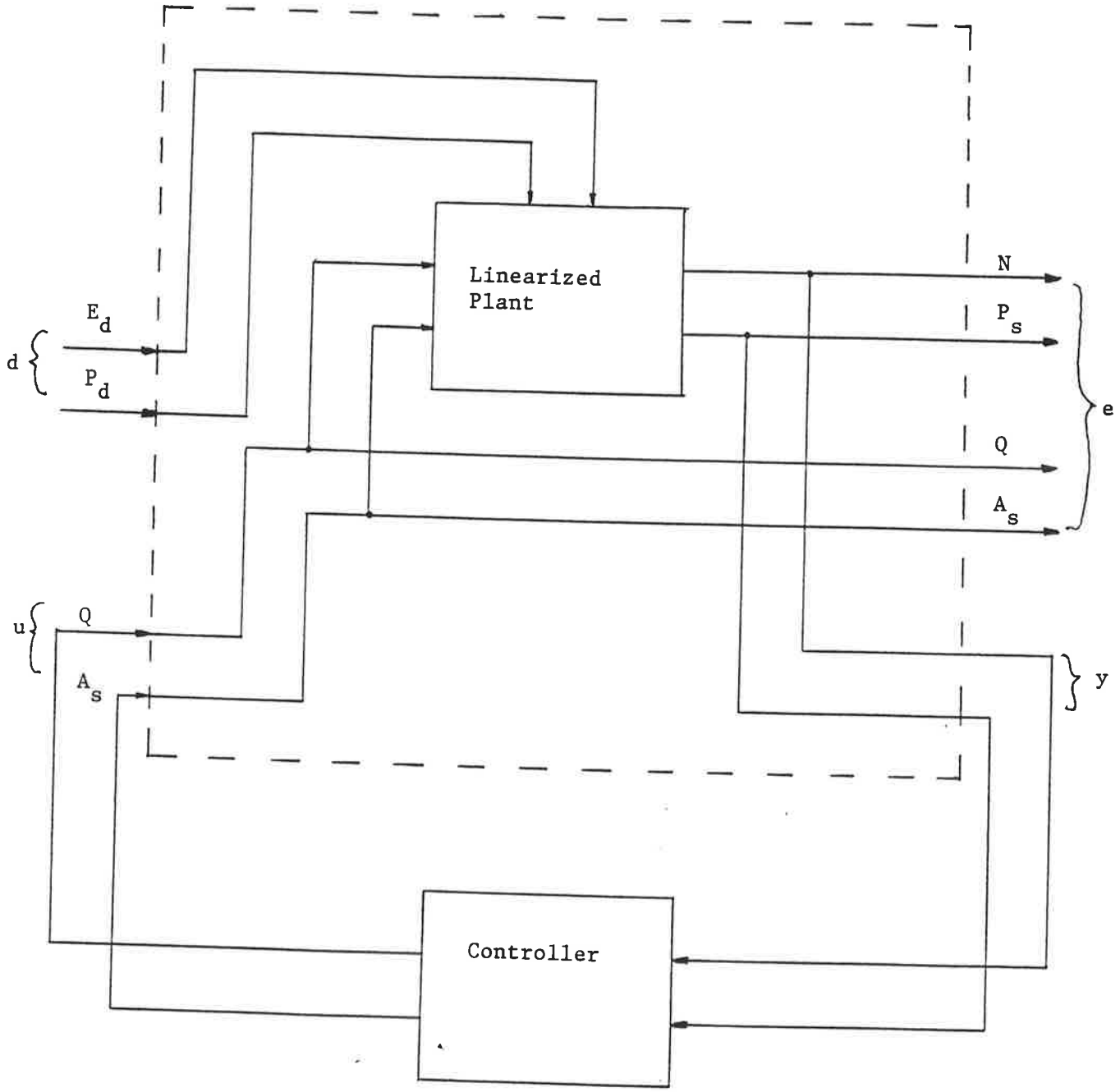

Fig. 9.

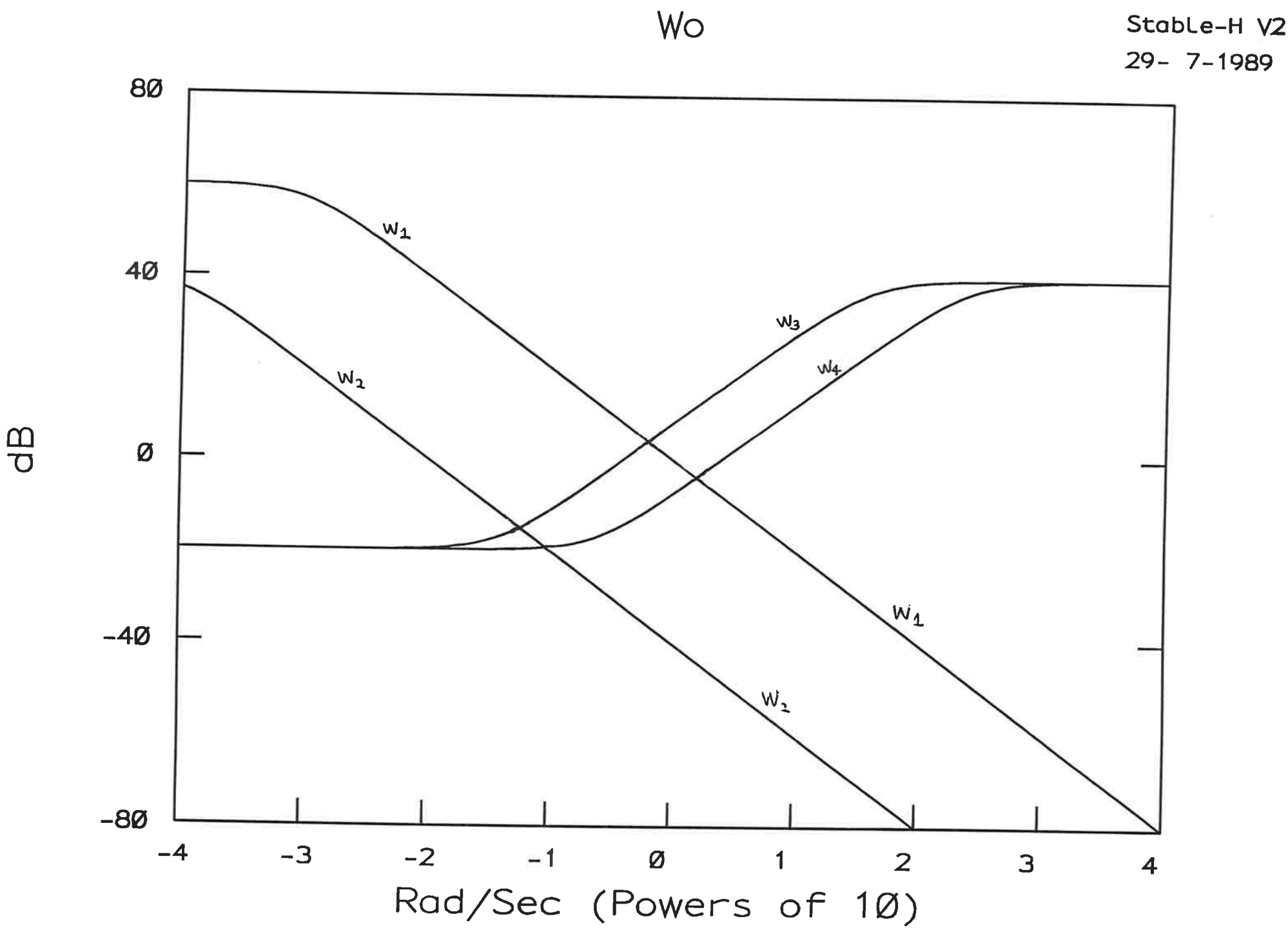
Wo
Stable-H V2
29- 7-1989
80
40
0
-40
-80
dB
W1
W2
W3
W4
W1
W2
-4
-3
-2
-1
0
1
2
3
4
Rad/Sec (Powers of 10)

Fig. 10

Resp. to +2% step in Ed

Stable-H V2
29- 7-1989

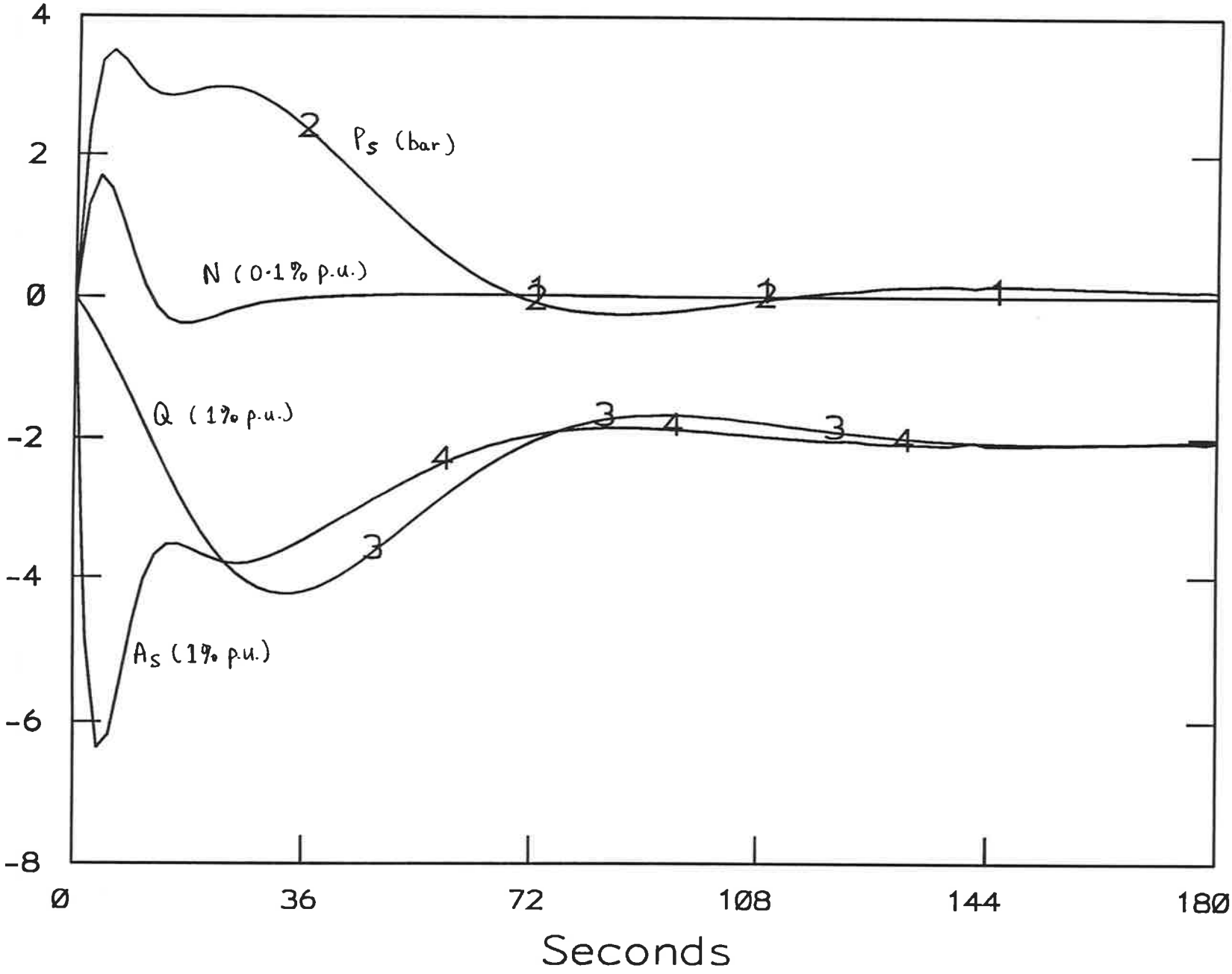

Fig. 11

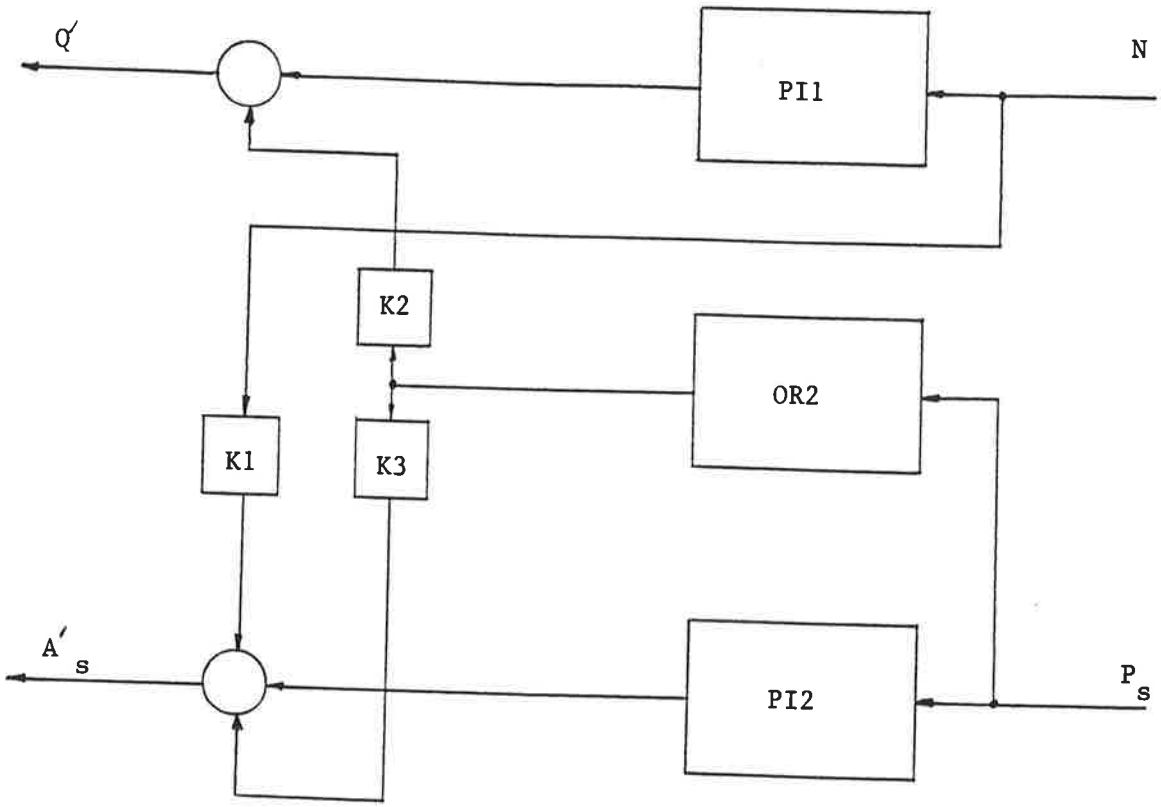

Fig. 12.